*Inorg. Chem.* **2002**, *41*, 28–33


# Trivalent Lanthanide Compounds with Fluorinated Thiolate Ligands: Ln–F Dative Interactions Vary with Ln and Solvent

**Jonathan H. Melman, Christa Rohde, Thomas J. Emge, and John G. Brennan***

*Department of Chemistry, Rutgers, the State University of New Jersey, 610 Taylor Road, Piscataway, New Jersey 08854-8087*

Received May 8, 2001

The fluorinated tris-thiolate compounds $Ln(SC_6F_5)_3$ can be isolated as THF, pyridine, or DME coordination complexes. In THF, the larger Ce forms dimeric $[(THF)_3Ce(SC_6F_5)_3]_2$ (**1**) with bridging thiolate ligands, while the smaller lanthanides (Ln = Ho (**2**), Er (**3**)) form monometallic $(THF)_3Ln(SC_6F_5)_3$ compounds. There is a tendency for fluoride to coordinate to Ln throughout the lanthanide series (Ce–Er). The cerium compound **1** contains a pair of bridging thiolates connecting two eight-coordinate Ce(III) ions. Of the two terminal thiolates, only one exhibits a distinct Ce–F bond. In contrast, the Ho derivative $(THF)_3Ho(SC_6F_5)_3$ is a molecular compound in the solid state, with two monodentate thiolates and one thiolate that again coordinates through both S and F atoms. Incorporation of a stronger Lewis base reduces but does not necessarily eliminate the tendency to form Ln–F bonds. Structural characterization of the eight-coordinate $(pyridine)_4Sm(SC_6F_5)_3$ (**4**) reveals a single, clearly defined Ln–F interaction, while in $(pyridine)_4Yb(SC_6F_5)_3$ (**5**) there are no Yb–F bonds. In the structure of $(DME)_2Er(SC_6F_5)_3$ (**6**) the DME ligands completely displace F from the Er coordination sphere.

## Introduction

Of the numerous lanthanide compounds containing fluorinated ligands that have been investigated for potential CVD applications,[1−3] there have been two reports[2,3] describing the synthesis of lanthanide compounds with organofluorine ligands that contain dative Ln−F interactions. Compounds with fluorinated amido ligands[2] were first communicated, and the dative Ln−F bonds noted in the solid state were found to be particularly susceptible to displacement by stronger Lewis base solvents. In contrast, with the more recently described fluorinated thiolate compounds, structural characterization of both divalent and trivalent $Ln(SC_6F_5)_x$ ($x$ = 2, 3) revealed that even in the presence of THF donors there were clear Ln−F interactions.[3] It was presumed that the geometric constraints imposed by the nearly 90° Ln−S−C angles in the thiolate compounds and the importance of $\pi$ stacking among the ligands were responsible for more pervasive Ln−F bonding in the thiolates.

Coordination of organofluoride ligands to metal ions is an unusual phenomenon.[4] Because of the weak, highly ionic nature of the M−F dative interaction, less electropositive metals (i.e., Hg, Pt) do not tend to form such bonds. With more electropositive metals there is a pronounced tendency either to have such bonds displaced by more strongly basic lone pairs or to engage in a C−F bond activation process that yields a metal fluoride compound.[4,5] The latter process is particularly prevalent in divalent Ln chemistry, where fluoride abstraction leads to oxidation of the Ln and the formation of fluoride compounds with a variety of ancillary ligands,[5] but activation of C−F bonds has also been noted in the thermal decomposition of the fluorinated thiolates.[3] As F coordination is presumably the first step in this C−F bond cleavage process, an understanding of dative Ln−F interactions would be helpful in developing new synthetic methods in organofluorine chemistry.

* Author to whom correspondence should be addressed. E-mail: bren@rutchem.rutgers.edu.

(1) (a) Malandrino, G.; Incontro, O.; Castelli, F.; Fragalà, I. L.; Benelli, C. *Chem. Mater*. **1996**, *8*, 1292. (b) Plakatouras, J. C.; Baxter, I.; Hursthouse, M. B.; Abdul Malik, K. M.; McAleese, J.; Drake, S. R. *J. Chem. Soc., Chem. Commun.* **1994**, 2455.
(2) Click, D. R.; Scott, B. L.; Watkin, J. G. *Chem. Commun.* **1999**, 633.
(3) Melman, J. H.; Emge, T. J.; Brennan, J. G. *Inorg. Chem.* **2001**, *40*, 1078.
(4) (a) Plenio, H. *Chem. Rev.* **1997**, *97*, 5553. (b) Murphy, E. F.; Murugavel, R.; Roesky, H. W. *Chem. Rev.* **1997**, *97*, 3425. (c) Kulawiec, R. J.; Crabtree, R. H. *Coord. Chem. Rev.* **1990**, *99*, 89. (d) Arroyo, M.; Bernes, S.; Brianso, J. L.; Mayoral, E.; Richards, R. L.; Ruis, J.; Torrens, H. *J. Organomet. Chem.* **2000**, *599*, 170.
(5) (a) Deacon, G. B.; Meyer, G.; Stellfeldt, D. *Eur. J. Inorg. Chem.* **2000**, 1061. (b) Deacon, G. B.; Harris, S. C.; Meyer, G.; Stellfeld, D.; Wilkinson, D. L.; Zelesny, G. *J. Organomet. Chem.* **1998**, *552*, 165. (c) Watson, P. L.; Tulip, T. H.; Williams, I. *Organometallics* **1990**, *9*, 1999. (d) Burns, C. J.; Berg, D. J.; Andersen, R. A. *J. Chem. Soc., Chem. Commun.* **1987**, 272. (e) Burns, C. J.; Andersen, R. A. *J. Chem. Soc., Chem. Commun.* **1989**, 136.



10.1021/ic0104813 CCC: $22.00 
Published on Web 12/06/2001

In this manuscript we outline the effect of neutral donor and Ln size on the tendency of $Ln(SC_6F_5)_3$ to form dative Ln−F interactions. THF coordination compounds of $Ce(SC_6F_5)_3$, $Ho(SC_6F_5)_3$, $Er(SC_6F_5)_3$, pyridine compounds of $Sm(SC_6F_5)_3$ and $Yb(SC_6F_5)_3$, and a DME coordination complex of $Er(SC_6F_5)_3$ are all examined in an effort to understand how the steric and electronic properties of neutral donors influence the Ln−F interaction.

## Experimental Section

**General Methods.** All syntheses were carried out under ultrapure nitrogen (JWS), using conventional drybox or Schlenk techniques. Solvents (Fisher) were refluxed continuously over molten alkali metals or K/benzophenone and collected immediately prior to use. Anhydrous pyridine (Aldrich) was purchased and refluxed over KOH. $Hg(SC_6F_5)_2$[3,6] was prepared according to literature procedure. Ln and Hg were purchased from Strem. $HSC_6F_5$ was purchased from Aldrich. Melting points were taken in sealed capillaries and are uncorrected. IR spectra were taken on a Mattus Cygnus 100 FTIR spectrometer and recorded from 4000 to 450 $cm^{-1}$ as a Nujol mull on KBr plates. Electronic spectra were recorded on a Varian DMS 100S spectrometer with the samples in a 1.0 mm or a 1.0 cm quartz cell attached to a Teflon stopcock. Molar absorptivities ($\epsilon$) are included in parentheses. Elemental analyses were performed by Quantitative Technologies, Inc. (Whitehouse, NJ). $^{19}F$ NMR and $^1H$ NMR spectra were obtained on a Varian Gemini 400 MHz NMR spectrometer, and chemical shifts are reported in $\delta$ (ppm). All products are unstable at room temperature for extended periods when dissolved in DME or pyridine.

**Synthesis of $[(THF)_3Ce(SC_6F_5)_3]_2$ (1).** Ce (0.176 g, 1.26 mmol) and $Hg(SC_6F_5)_2$ (1.13 g, 1.89 mmol) were combined in THF (20 mL), and the mixture was stirred until the chunks of metal were consumed and elemental mercury was visible in the bottom of the flask (overnight). The pale yellow solution was filtered away from the mercury (0.32 g, 84%), reduced in volume under vacuum to ca. 15 mL, and layered with hexane (15 mL) to give colorless crystals (0.732 g, 61%) which turn an opaque white at 93 °C, melt at 217−226 °C, appear to eliminate a gas at 278 °C, begin to darken at 297 °C, and continue to darken up to 350 °C. IR: 2923 (s), 2854 (s), 1502 (m), 1464 (s), 1378 (m), 1317 (w), 1299 (w), 1262 (w), 1171 (w), 1139 (w), 1126 (w), 1079 (m), 1069 (m), 1009 (m), 971 (m), 921 (w), 859 (m), 748 (w), 723 (w), 664 (w) $cm^{-1}$. UV−vis (THF): no absorption maxima, but slow diffusion of air into the sample gave an absorption centered at 430 nm ($\epsilon$ > 200 (M $cm)^{-1}$). Anal.Calcd for $C_{60}H_{48}Ce_2F_{30}O_6$: C, 37.8; H, 2.54. Found: C, 37.0; H, 2.50. $^{19}F$ NMR ($OC_4D_8$, 24 °C): −131.4 (2F, d, $J$ = 20 Hz), −148.4 (2F, t, $J$ = 21 Hz), −159.9 (1F, t, $J$ = 21 Hz).

**Synthesis of $(THF)_3Ho(SC_6F_5)_3$ (2).** As for **1** above, Ho (0.244 g, 1.48 mmol) and $Hg(SC_6F_5)_2$ (1.327 g, 2.219 mmol) in THF (ca. 25 mL) gave mercury (0.37 g, 82%) and pink crystals (0.373 g, 26%) that turn white and appear to lose solvent at 183 °C, melt between 217 and 240 °C, and appeared to eliminate a gas at 273 °C. IR: 2947 (s), 2871 (s), 1504 (m), 1462 (s), 1378 (s), 1300 (w), 1262 (w), 1173 (w), 1125 (w), 1083 (m), 1069 (m), 1039 (w), 1006 (m), 967 (m), 925 (w), 895 (w), 859 (m), 723 (w), 669 (w), 619 (w) $cm^{-1}$. UV−vis (in THF): 362 (18), 421 (5.1), 451 (68), 457 (29), 462 (24), 539 (3.6), 552 (2.2), 642 (1.8). Anal. Calcd for $C_{30}H_{24}F_{15}HoO_3S_3$: C, 36.8; H, 2.47. Found: C, 36.3; H, 2.42. $^{19}F$ NMR ($OC_4D_8$, 24 °C): −179.6 (2 F, $w_{1/2}$ = 76 Hz), −181.5 (1 F, $w_{1/2}$ = 53 Hz). There was no change in line shape as a function of temperature.

(6) Peach, M. E. *J. Inorg. Nucl. Chem.* **1973**, *35*, 1046.

**Synthesis of $(THF)_3Er(SC_6F_5)_3$ (3).** As for **1** above, Er (0.191 g, 1.14 mmol) and $Hg(SC_6F_5)_2$ (1.02 g, 1.71 mmol) in THF (ca. 30 mL) gave mercury (0.33 g, 97%) and pink crystals (0.396 g, 35%) that become opaque at 100 °C, begin to darken at 170 °C, and turn black by 328 °C. IR: 2945 (s), 2875 (s), 1505 (m), 1462 (s), 1378 (s), 1301 (w), 1264 (w), 1173 (w), 1124 (w), 1083 (m), 1070 (m), 1006 (m), 967 (m), 927 (w), 859 (m), 724 (w), 670 (w), 620 (w) $cm^{-1}$. Unit cell (Mo Kα, 153 K): space group $P2_1/n$, $a$ = 12.03(1) Å, $b$ = 22.13(1) Å, $c$ = 12.65(1) Å, $\beta$ = 97.54(7)°, $Z$ = 4, $V$ = 3339(4) $Å^3$. UV−vis (THF): 367 (2.5), 380 (37), 385 (14), 490 (1.6) 522 (19), 654 (1.3). Anal. Calcd for $C_{30}H_{24}ErF_{15}O_3S_3$: C, 36.7; H, 2.47. Found: C, 36.7; H, 2.52. $^{19}F$ NMR (24 °C, $OC_4D_8$): −161.4 (1F, $w_{1/2}$ = 49 Hz), −152.8 (2F, $w_{1/2}$ = 62 Hz), −96.3 (2F, $w_{1/2}$ = 645 Hz). When heated at 220 °C under vacuum, the compound eliminates white crystalline material that was identified as a mixture of $(C_6F_2S)_2$ and $(C_6F_4S)_n$ ($n$ = 2, 3) by DP-EI-MS. XRPD identified $ErF_3$ as the only crystalline Er product.

**Synthesis of $(py)_4Sm(SC_6F_5)_3 \cdot {}^1/_2py$ (4).** As for **1**, Sm (0.215 g, 1.43 mmol) and $Hg(SC_6F_5)_2$ (1.29 g, 2.16 mmol) in pyridine (10 mL) gave mercury (0.39 g, 93%) and, when cooled (5 °C), yellow crystals (0.325 g, 35%) that start turning red at 60 °C, show some signs of melting at 64 °C, and start turning black at 105 °C. IR: 2924 (s), 2855 (s), 1512 (m), 1498 (s), 1465 (s), 1378 (m), 1261 (m), 1090 (s), 1021 (m), 967 (m), 921 (w), 899 (w), 866 (m), 841 (w), 805 (m), 751 (w), 724 (w), 701 (m), 673 (w), 663 (w), 623 (w) $cm^{-1}$. UV−vis (toluene) shows only the visible tail of a UV absorption. Anal. Calcd for $C_{40.5}H_{22.5}F_{15}N_{4.5}S_3Sm_1$: C, 44.1; H, 2.05; N, 5.71. Found: C, 44.5; H, 2.38; N, 6.30. $^{19}F$ NMR ($OC_4D_8$, 24 °C): −132.5 (2F, $w_{1/2}$ = 69 Hz), −161.9 (1F, $w_{1/2}$ = 74 Hz).

**Synthesis of $Yb(SC_6F_5)_3(pyr)_4 \cdot pyr \cdot THF$ (5)**. Yb (0.214 g, 1.24 mmol) and $Hg(SC_6F_5)_2$ (1.109 g, 1.855 mmol) were combined in THF (ca. 25 mL). The solution was stirred until the metal was consumed, and only mercury was visible on the bottom of the reaction mixture (ca. 1 day). The red solution was filtered, pyridine (5 mL, 60 mmol) was added, and the mixture was layered with 20 mL of hexane and cooled to 5 °C to give red-orange crystals (1.357 g, 88%) that turn red and melt between 79 and 84 °C. Above 135 °C the liquid deposits a yellow-orange solid that darkens at 169 °C. IR: 2926 (s), 2857 (s), 1604 (m), 1504 (m), 1464 (s), 1378 (s), 1264 (w), 1223 (m), 1157 (w), 1072 (m), 1040 (w), 1006 (m), 968 (m), 916 (w), 859 (m), 758 (m), 701 (m), 626 (w) $cm^{-1}$. UV−vis (pyr): 440 nm (273 $M^{-1}$ $cm^{-1}$), with a shoulder at 400 nm. Anal. Calcd for $C_{47}H_{33}YbF_{15}OS_3$: C, 45.6; H, 2.69; N, 5.66. Found: C, 44.6; H, 2.58; N, 5.57. $^{19}F$ NMR ($C_6D_6$, 24 °C): −108.7 ppm (2F, $w_{1/2}$ = 252 Hz), −160.0 ppm (2F, $w_{1/2}$ = 95 Hz), −160.9 (1F, $w_{1/2}$ = 95 Hz). $^1H$ NMR ($C_6D_6$, 24 °C): 8.60 (10H, $w_{1/2}$ = 193 Hz), 4.01 (4H, $w_{1/2}$ = 101 Hz), 1.57 (4H, $w_{1/2}$ = 28 Hz). Assignments of the proton resonances were deduced by addition of THF or pyridine. There is no change in the $^{19}F$ NMR spectrum upon addition of sulfur to the NMR tube. When dissolved in pyridine or DME, **5** decomposes thermally at room temperature to give a colorless solution and a light yellow, insoluble precipitate.

**Synthesis of $(DME)_2Er(SC_6F_5)_3$ (6).** As for **1** above, Er (0.193 g, 1.15 mmol) and $Hg(SC_6F_5)_2$ (1.035 g, 1.731 mmol) in DME (ca. 20 mL) gave mercury (0.30 g, 87%) and pink crystals (0.827 g, 73%) that turn yellow at 79 °C, melt and turn orange at 215 °C, and blacken at 257 °C. IR: 2923 (s), 2854 (s), 1506 (m), 1465 (s), 1378 (m), 1260 (m), 1189 (w), 1084 (m), 1075 (m), 1030 (m), 986 (w), 967 (m), 907 (w), 866 (m), 856 (m), 803 (w), 722 (w) $cm^{-1}$. UV−vis (THF): 367 (2.5), 380 (27), 490 (1.3), 522 (15), 653 (1.0). Anal. Calcd for $C_{26}H_{20}ErF_{15}O_4S_3$: C, 33.0; H, 2.13. Found: C, 32.5; H, 1.94. The $^{19}F$ NMR ($C_6D_6$, 24 °C) resonances could not be located.

**Table 1.** Summary of Crystallographic Details for **1**, **2**, and **4**−**6**

| | **1** | **2** | **4** | **5** | **6** |
|---|---|---|---|---|---|
| empirical formula | $C_{30}H_{24}CeF_{15}O_3S_3$ | $C_{30}H_{24}F_{15}HoO_3S_3$ | $C_{40.5}H_{22.5}F_{15}N_{4.5}S_3Sm$ | $C_{47}H_{33}F_{15}N_5OS_3Yb$ | $C_{26}H_{20}ErF_{15}O_4S_3$ |
| fw | 953.79 | 978.60 | 1103.66 | 1238.00 | 944.86 |
| space group | $P\bar{1}$ | $P2_1/n$ | $P\bar{1}$ | $P2_1/n$ | $C2/c$ |
| $a$ (Å) | 11.055(5) | 12.004(5) | 9.510(3) | 11.513(7) | 33.071(7) |
| $b$ (Å) | 12.377(5) | 22.247(11) | 14.644(5) | 31.499(8) | 8.9410(15) |
| $c$ (Å) | 13.216(6) | 12.697(4) | 15.911(9) | 14.144(5) | 21.544(3) |
| α (deg) | 71.77(3) | 90.00 | 108.96(4) | 90.00 | 90.00 |
| $\beta$ (deg) | 76.36(4) | 97.71(3) | 92.21(3) | 112.23(4) | 90.46(1) |
| $\gamma$ (deg) | 84.90(3) | 90.00 | 95.00(3) | 90.00 | 90.00 |
| $V$ (Å$^3$) | 1669(1) | 3360(2) | 2082(1) | 4748(4) | 6370(2) |
| $Z$ | 2 | 4 | 2 | 4 | 8 |
| $D$(calcd) (g/cm$^{-3}$) | 1.898 | 1.934 | 1.760 | 1.732 | 1.970 |
| temp (°C) | −120 | −120 | −120 | −120 | −120 |
| $\lambda$ (Å) | 0.71073 | 0.71073 | 0.71073 | 0.71073 | 0.71073 |
| abs coeff (mm$^{-1}$) | 1.669 | 2.658 | 1.665 | 2.204 | 2.953 |
| $R(F)^a$ [$I > 2\sigma(I)$] | 0.029 | 0.024 | 0.056 | 0.024 | 0.025 |
| $R_w(F^2)^a$ [$I > 2\sigma(I)$] | 0.073 | 0.054 | 0.112 | 0.056 | 0.063 |

[a] Definitions: $R(F) = \sum||F_o| - |F_c||/\sum|F_o|$; $R_w(F^2) = \{\sum[w(F_o^2 - F_c^2)^2]/\sum[w(F_o^2)^2]\}^{1/2}$. Additional crystallographic details are given in the Supporting Information.

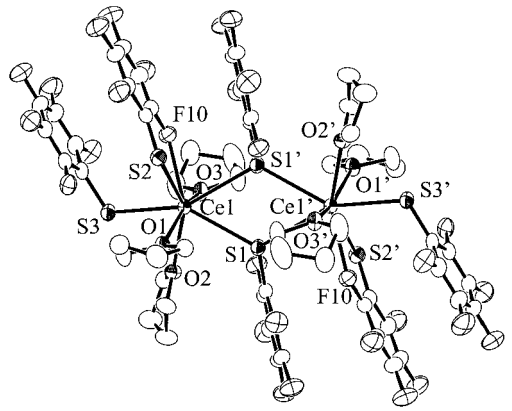


**Figure 1.** ORTEP diagram of $[(THF)_3Ce(SC_6F_5)_3]_2$ (**1**). Thermal ellipsoids are drawn at the 50% probability level.

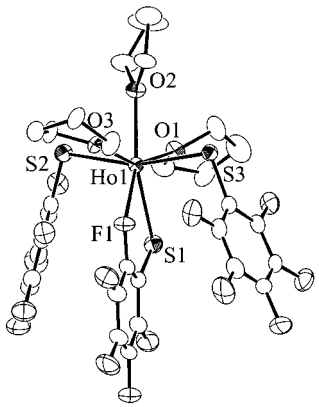


**Figure 2.** ORTEP diagram of $(THF)_3Ho(SC_6F_5)_3$ (**2**). Thermal ellipsoids are drawn at the 50% probability level.

**X-ray Structure Determination of 1, 2, and 4−6.** Data for **1**, **2**, and **4**−**6** were collected on an Enraf-Nonius CAD4 diffractometer with graphite-monochromatized Mo Kα radiation ($\lambda$ = 0.71073 Å) at −120 °C. The three check reflections, measured every hour, showed less than 2% intensity variation. The data were corrected for Lorentz effects and polarization, and absorption, the latter by a numerical (SHELX76)[7] method. The structures were solved by direct methods (SHELXS86).[8] All non-hydrogen atoms were refined (SHELXL97)[9] based upon $F_{obs}^2$. All hydrogen atom coordinates were calculated with idealized geometries. Scattering factors ($f_o$, $f'$, $f''$) are as described in SHELXL97. Crystallographic data and final $R$ indices for **1**, **2**, and **4**−**6** are given in Table 1. Significant bond distances and angles for **1**, **2**, and **4**−**6** are given in the figure captions. Complete crystallographic details are given in the Supporting Information. ORTEP diagrams[10] for **1**, **2**, and **4**−**6** are shown in Figures 1−5, respectively.

## Results

Transmetalation reactions of Ln (Ln = Ce, Sm, Ho, Er, Yb) with $Hg(SC_6F_5)_2$ in THF, pyridine, or DME give the corresponding trivalent thiolates in 26−88% isolated, crystalline yields (reaction 1). Colorless $[(THF)_3Ce(SC_6F_5)_3]_2$ (**1**)

$$2Ln + 3Hg(SC_6F_5)_2 \xrightarrow{\text{solvent}} 2(\text{solvent})_xLn(SC_6F_5)_3 + 3Hg \quad (1)$$

is a dimer, with a pair of bridging thiolates connecting two eight-coordinate Ce(III) ions, with four sulfur atoms, three oxygen atoms, and one fluorine atom comprising the primary coordination sphere. Figure 1 shows an ORTEP diagram of **1**, and Table 2 gives a listing of significant bond distances and angles for **1**. The shortest Ce−F separation is the 2.749(2) Å dative interaction between Ce and F(10), and there are $\pi-\pi$ interactions between the S(2) and S(3) thiolates, as in Figure 1. With smaller Ln, there is an increasing tendency to form monometallic structures. The THF derivatives of both $Ho(SC_6F_5)_3$ (**2**) and $Er(SC_6F_5)_3$ (**3**) are isostructural, and a complete structural analysis of the Ho compound $(THF)_3Ho(SC_6F_5)_3$ reveals a pentagonal bipyramidal product with two axial thiolates and one equatorial thiolate. The structure of **2** is shown in Figure 2, and

(7) Sheldrick, G. M. *SHELX76, Program for Crystal Structure Determination*; University of Cambridge: Cambridge, England, 1976.
(8) Sheldrick, G. M. *SHELXS86, Program for the Solution of Crystal Structures*; University of Göttingen: Göttingen, Germany, 1986.
(9) Sheldrick, G. M. *SHELXL97, Program for Crystal Structure Refinement*; University of Göttingen: Göttingen, Germany, 1997.
(10) (a) Johnson, C. K. *ORTEP II*; Report ORNL-5138; Oak Ridge National Laboratory: Oak Ridge, TN, 1976. (b) Zsolnai, L. *XPMA and ZORTEP, Programs for Interactive ORTEP Drawings*; University of Heidelberg: Heidelberg, Germany, 1997.

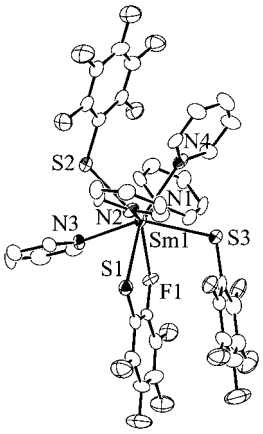


**Figure 3.** ORTEP diagram of $(py)_4Sm(SC_6F_5)_3$ (**4**). Thermal ellipsoids are drawn at the 50% probability level.

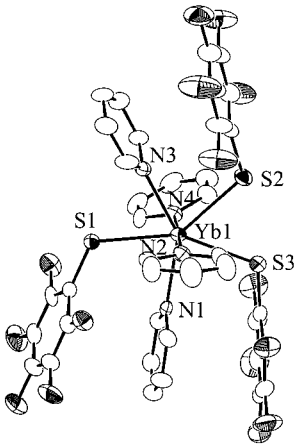


**Figure 4.** ORTEP diagram of $(py)_4Yb(SC_6F_5)_3$ (**5**). Thermal ellipsoids are drawn at the 50% probability level.

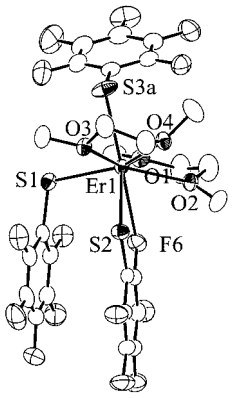


**Figure 5.** ORTEP diagram of $(DME)_2Er(SC_6F_5)_3$ (**6**). Thermal ellipsoids are drawn at the 50% probability level.

significant bond distances and angles are given in Table 3. The equatorial thiolate ligand coordinates through both S(1) and F(1) donor interactions, with a Ho−F(1) distance of 2.579(2) Å, as in Figure 2.

Pyridine complexes of $Ln(C_6F_5)_3$ have similar structural features. In both $(py)_4Sm(SC_6F_5)_3$ (**4**) and $(py)_4Yb(SC_6F_5)_3$ (**5**), the presence of the stronger neutral pyridine donor results in the formation of monometallic compounds with only terminal thiolate ligands. ORTEP diagrams for **4** and **5** are given in Figures 3 and 4 respectively, and significant bond geometries are given in Tables 4 and 5, respectively. In the

**Table 2.** Bond Lengths (Å) and Angles (deg) for $[(THF)_3Ce(SC_6F_5)_3]_2$

| | | | |
|---|---|---|---|
| Ce(1)−O(3) | 2.509(3) | Ce(1)−S(3) | 2.8567(17) |
| Ce(1)−F(10) | 2.749(2) | Ce(1)−S(1)′ | 3.0381(19) |
| Ce(1)−S(1) | 3.0089(16) | Ce(1)−O(2) | 2.554(3) |
| Ce(1)−O(1) | 2.516(3) | Ce(1)−S(2) | 2.8696(16) |
| O(3)−Ce(1)−O(1) | 158.03(9) | O(3)−Ce(1)−O(2) | 81.62(9) |
| O(1)−Ce(1)−O(2) | 76.46(9) | O(3)−Ce(1)−F(10) | 65.09(8) |
| O(1)−Ce(1)−F(10) | 131.65(8) | O(2)−Ce(1)−F(10) | 134.30(8) |
| O(3)−Ce(1)−S(3) | 84.35(7) | O(1)−Ce(1)−S(3) | 86.70(7) |
| O(2)−Ce(1)−S(3) | 69.87(7) | F(10)−Ce(1)−S(3) | 76.23(6) |
| O(3)−Ce(1)−S(2) | 129.06(7) | O(1)−Ce(1)−S(2) | 70.70(7) |
| O(2)−Ce(1)−S(2) | 141.95(7) | F(10)−Ce(1)−S(2) | 64.31(6) |
| S(3)−Ce(1)−S(2) | 89.29(5) | O(3)−Ce(1)−S(1) | 92.28(7) |
| O(1)−Ce(1)−S(1) | 83.84(7) | O(2)−Ce(1)−S(1) | 75.66(7) |
| F(10)−Ce(1)−S(1) | 132.81(6) | S(3)−Ce(1)−S(1) | 145.50(3) |
| S(2)−Ce(1)−S(1) | 118.23(4) | O(3)−Ce(1)−S(1)′ | 86.46(7) |
| O(1)−Ce(1)−S(1)′ | 109.33(7) | O(2)−Ce(1)−S(1)′ | 131.76(7) |
| F(10)−Ce(1)−S(1)′ | 78.55(6) | S(3)−Ce(1)−S(1)′ | 154.74(3) |
| S(2)−Ce(1)−S(1)′ | 78.40(5) | S(1)−Ce(1)−S(1)′ | 58.25(5) |
| C(1)−S(1)−Ce(1) | 119.33(12) | | |

**Table 3.** Bond Lengths (Å) and Angles (deg) for $(THF)_3Ho(SC_6F_5)_3$

| | | | |
|---|---|---|---|
| Ho(1)−O(1) | 2.341(2) | Ho(1)−S(3) | 2.7111(14) |
| Ho(1)−F(1) | 2.579(2) | Ho(1)−O(2) | 2.375(2) |
| Ho(1)−S(1) | 2.7241(14) | Ho(1)−S(2) | 2.7169(14) |
| Ho(1)−O(3) | 2.375(2) | | |
| O(1)−Ho(1)−O(3) | 153.45(8) | O(1)−Ho(1)−O(2) | 77.00(8) |
| O(3)−Ho(1)−O(2) | 76.45(8) | O(1)−Ho(1)−F(1) | 140.85(7) |
| O(3)−Ho(1)−F(1) | 64.58(7) | O(2)−Ho(1)−F(1) | 138.31(7) |
| O(1)−Ho(1)−S(3) | 88.38(7) | O(3)−Ho(1)−S(3) | 89.14(6) |
| O(2)−Ho(1)−S(3) | 83.54(7) | F(1)−Ho(1)−S(3) | 81.71(6) |
| O(1)−Ho(1)−S(2) | 86.97(7) | O(3)−Ho(1)−S(2) | 88.16(6) |
| O(2)−Ho(1)−S(2) | 80.42(7) | F(1)−Ho(1)−S(2) | 111.24(6) |
| S(3)−Ho(1)−S(2) | 163.92(3) | O(1)−Ho(1)−S(1) | 76.53(7) |
| O(3)−Ho(1)−S(1) | 129.94(6) | O(2)−Ho(1)−S(1) | 153.39(6) |
| F(1)−Ho(1)−S(1) | 67.74(5) | S(3)−Ho(1)−S(1) | 98.45(4) |
| S(2)−Ho(1)−S(1) | 95.42(5) | C(1)−S(1)−Ho(1) | 106.14(11) |

**Table 4.** Bond Lengths (Å) and Angles (deg) for $(py)_4Sm(SC_6F_5)_3$

| | | | |
|---|---|---|---|
| Sm(1)−N(2) | 2.561(7) | Sm(1)−F(1) | 2.703(5) |
| Sm(1)−N(4) | 2.619(7) | Sm(1)−S(2) | 2.867(3) |
| Sm(1)−S(1) | 2.831(3) | Sm(1)−N(1) | 2.615(7) |
| Sm(1)−N(3) | 2.581(7) | Sm(1)−S(3) | 2.809(3) |
| N(2)−Sm(1)−N(3) | 109.6(3) | N(2)−Sm(1)−N(1) | 158.1(2) |
| N(3)−Sm(1)−N(1) | 83.6(2) | N(2)−Sm(1)−N(4) | 78.1(2) |
| N(3)−Sm(1)−N(4) | 142.1(2) | N(1)−Sm(1)−N(4) | 80.9(2) |
| N(2)−Sm(1)−F(1) | 134.7(2) | N(3)−Sm(1)−F(1) | 68.4(2) |
| N(1)−Sm(1)−F(1) | 66.0(2) | N(4)−Sm(1)−F(1 | 132.8(2) |
| N(2)−Sm(1)−S(3) | 92.08(19) | N(3)−Sm(1)−S(3) | 144.42(18) |
| N(1)−Sm(1)−S(3) | 86.00(17) | N(4)−Sm(1)−S(3) | 68.38(17) |
| F(1)−Sm(1)−S(3) | 76.29(12) | N(2)−Sm(1)−S(1) | 69.71(18) |
| N(3)−Sm(1)−S(1) | 75.98(17) | N(1)−Sm(1)−S(1) | 131.79(17) |
| N(4)−Sm(1)−S(1) | 137.94(16) | F(1)−Sm(1)−S(1) | 65.96(12) |
| S(3)−Sm(1)−S(1) | 86.19(8) | N(2)−Sm(1)−S(2) | 83.78(18) |
| N(3)−Sm(1)−S(2) | 65.89(18) | N(1)−Sm(1)−S(2) | 85.97(18) |
| N(4)−Sm(1)−S(2) | 78.71(17) | F(1)−Sm(1)−S(2) | 128.26(12) |
| S(3)−Sm(1)−S(2) | 146.95(7) | S(1)−Sm(1)−S(2) | 122.21(8) |
| C(1)−S(1)−Sm(1) | 106.4(3) | | |

structure of eight-coordinate **4** (4N, 3S, 1F) there is a single Sm−F dative interaction with a 2.703(5) Å Sm−F(1) separation (Figure 3), and there are clear $\pi-\pi$ interactions[11] of pyridine (N4)/thiolate (S2), and between two thiolate ligands (S(1) and S(3)). In the pyridine complex of the smaller Yb(III) ion the coordination number has been reduced to seven (4 nitrogen, 3 sulfur) to produce a pentagonal bipyramidal geometry with two axial pyridine ligands, three

(11) Coates, G. W.; Dunn, A. R.; Henling, L. M.; Dougherty, D. A.; Grubbs, R. H. *Angew. Chem., Int. Ed. Engl.* **1997**, *36*, 248.

**Table 5.** Bond Lengths (Å) and Angles (deg) for $(py)_4Yb(SC_6F_5)_3$

| | | | |
|---|---|---|---|
| Yb(1)−N(3) | 2.424(3) | Yb(1)−S(2) | 2.752(1) |
| Yb(1)−N(1) | 2.466(3) | Yb(1)−N(2) | 2.457(3) |
| Yb(1)−S(3) | 2.763(2) | Yb(1)−S(1) | 2.760(2) |
| Yb(1)−N(4) | 2.437(3) | | |
| N(3)−Yb(1)−N(4) | 89.16(9) | N(3)−Yb(1)−N(2) | 94.58(10) |
| N(4)−Yb(1)−N(2) | 176.11(9) | N(3)−Yb(1)−N(1) | 141.42(9) |
| N(4)−Yb(1)−N(1) | 88.73(10) | N(2)−Yb(1)−N(1) | 89.02(10) |
| N(3)−Yb(1)−S(2) | 76.30(7) | N(4)−Yb(1)−S(2) | 89.95(7) |
| N(2)−Yb(1)−S(2) | 89.87(7) | N(1)−Yb(1)−S(2) | 142.21(7) |
| N(3)−Yb(1)−S(1) | 141.57(7) | N(4)−Yb(1)−S(1) | 87.11(8) |
| N(2)−Yb(1)−S(1) | 89.27(8) | N(1)−Yb(1)−S(1) | 76.74(7) |
| S(2)−Yb(1)−S(1) | 65.47(4) | N(3)−Yb(1)−S(3) | 76.17(7) |
| N(4)−Yb(1)−S(3) | 92.19(8) | N(2)−Yb(1)−S(3) | 89.77(8) |
| N(1)−Yb(1)−S(3) | 65.43(7) | S(2)−Yb(1)−S(3) | 152.35(3) |
| S(1)−Yb(1)−S(3) | 142.17(4) | C(1)−S(1)−Yb(1) | 115.85(11) |

**Table 6.** Bond Lengths (Å) and Angles (deg) for $(DME)_2Er(SC_6F_5)_3$

| | | | |
|---|---|---|---|
| Er(1)−O(2) | 2.384(2) | Er(1)−S(3A) | 2.6942(16) |
| Er(1)−O(3) | 2.467(2) | Er(1)−S(2) | 2.7215(10) |
| Er(1)−S(3B) | 2.700(8) | Er(1)−O(4) | 2.452(2) |
| Er(1)−O(1) | 2.409(2) | Er(1)−S(1) | 2.7004(9) |
| O(2)−Er(1)−O(1) | 66.25(9) | O(2)−Er(1)−O(4) | 70.66(8) |
| O(1)−Er(1)−O(4) | 121.18(8) | O(2)−Er(1)−O(3) | 134.49(8) |
| O(1)−Er(1)−O(3) | 151.99(8) | O(4)−Er(1)−O(3) | 65.90(8) |
| O(2)−Er(1)−S(3A) | 114.40(8) | O(1)−Er(1)−S(3A) | 83.47(7) |
| O(4)−Er(1)−S(3A) | 79.80(7) | O(3)−Er(1)−S(3A) | 70.81(7) |
| O(2)−Er(1)−S(1) | 139.38(6) | O(1)−Er(1)−S(1) | 84.36(7) |
| O(4)−Er(1)−S(1) | 149.54(6) | O(3)−Er(1)−S(1) | 83.78(6) |
| S(3A)−Er(1)−S(1) | 87.80(5) | O(2)−Er(1)−S(3B) | 101.84(19) |
| O(1)−Er(1)−S(3B) | 79.07(16) | O(4)−Er(1)−S(3B) | 72.64(18) |
| O(3)−Er(1)−S(3B) | 77.90(17) | S(3A)−Er(1)−S(3B) | 12.69(17) |
| S(1)−Er(1)−S(3B) | 99.14(18) | O(2)−Er(1)−S(2) | 86.68(7) |
| O(1)−Er(1)−S(2) | 131.23(6) | O(4)−Er(1)−S(2) | 82.06(6) |
| O(3)−Er(1)−S(2) | 74.77(6) | S(3A)−Er(1)−S(2) | 145.24(4) |
| S(1)−Er(1)−S(2) | 93.19(3) | S(3B)−Er(1)−S(2) | 148.51(15) |
| C(1)−S(1)−Er(1) | 107.44(11) | | |

terminal equatorial thiolates, and no Ln−F bonds (Figure 4). In the Yb structure **5** there are significant $\pi-\pi$ stacking interactions between the S(2) and S(3) thiolates and a sandwiched pyridine (N1), as well as $\pi-\pi$ interactions between the S(2) thiolate and a pyridine (N3) ligand. The compound has an intense visible absorption band with a maximum at 440 nm that can be assigned as a S to Yb charge transfer absorption on the basis of earlier resonance Raman measurements.[12]

Because of the solubilizing tendency of these fluorinated ligands, transmetalation reactions of Ln with $Hg(SC_6F_5)_2$ will run to completion in solvents as apolar as DME. Transmetalation of $Hg(SC_6F_5)_2$ with Er in DME gives the first structurally characterized Er thiolate $(DME)_2Er(SC_6F_5)_3$ (**6**). An ORTEP diagram of this compound is given in Figure 5, and significant bond geometries are given in Table 6. There is only one thiolate (S2) that could possibly be viewed as coordinating through both S and F atoms, with a comparatively long 2.948(6) Å Er−F(6) separation. In this compound the one thiolate (S2) with the closest Er−F interaction is positioned to interact strongly with the neighboring $\pi$ system on the ring attached to S1. This compound decomposes thermally to form $ErF_3$, $(SC_6F_5)_2$, and $(SC_6F_4)_x$ ($x = 2, 3$).

## Discussion

This diverse array of $Ln(SC_6F_5)_3$ coordination complexes complements the initially reported[3] syntheses and structures of divalent $[(THF)_2Eu(SC_6F_5)_2]_n$ and trivalent $[(THF)_2Sm(SC_6F_5)_3]_2$, and clearly demonstrates how the chemical and physical properties of compounds with fluorinated thiolate ligands differ from those of their $SC_6H_5$ counterparts. A most dramatic effect is the tendency of fluorinated thiolate ligands to form complexes with reduced nuclearity. While benzenethiolate compounds of the early lanthanides form polymeric structures with metals as small as Sm(III),[12] the corresponding fluorinated derivatives are either dimeric products or molecular species with Ln−F interactions serving to complete the lanthanide coordination sphere. Reduced nuclearity is a direct consequence of the fluorine substitution, which reduces S basicity by polarizing electron density away from S and into the arene functional group. The best example of this effect comes from the Sm structures, where coordination complexes of $L_xSm(SC_6F_5)_3$ have consistently lower nuclearity (dimer, L = THF;[3] monomer, L = pyridine) than their $L_xSm(SPh)_3$ counterparts[12] (polymer, L = THF; tetramer, L = pyridine). In both cases, the more basic pyridine ligand is better able to disrupt Ln−S(R)−Ln bridging interactions.

Because Ln−F interactions are weak and thus readily distorted, it is difficult to establish exactly what constitutes a Ln−fluoride dative interaction. Assessments based on comparisons between interatomic distances and van der Waals radii are impossible because there are no values available for the lanthanide ions. Still, relatively short Ln−F separations can be interpreted by comparison with published values for the van der Waals radii[13] of F (1.47 Å) and O (1.52 Å) or N (1.55 Å), and the abundance of dative Ln−O(THF) or Ln−N (pyridine) bonds in the structures reported here. In the majority of cases, the Ln−F is ca. 0.1−0.2 Å longer than the average bonds to either THF or pyridine: in **1** (Ce−O = 2.53 Å, Ce−F = 2.75 Å), **2** (Ho−O = 2.36 Å, Ho−F = 2.58 Å), or **4** (Sm−N = 2.59 Å, Sm−F = 2.70 Å). As such, these are clearly Ln−F interactions. Less well defined is the Ln−F interaction in **6**, where the average Er−O bond is 2.43(2) Å but the Er−F(6) distance is 2.945(5) Å. In this case, a significant Er−F interaction can be discounted by comparison of Er−S bonds in **6** relative to the Ho−S bonds in **2**; the Ho−S bond lengths average 0.01 Å longer than the Er−S bond lengths. This difference is precisely that expected from ionic radius summation arguments, and therefore both Ln effectively have the same coordination number (7): Ho (3S, 3O, 1F); Er (3S, 4O).

Substitution of SPh by $SC_6F_5$ appears to influence the length of the Ln−S bond. Comparisons are difficult, because structurally characterized tris-benzenethiolate compounds of the lanthanide elements represent a small family of compounds (including $[(THF)Sm(SPh)_3]_n$,[12] $[(py)_2Sm(SPh)_3]_4$,[12] $(hmpa)_3Ln(SPh)_3$ (Ln = Sm, Yb),[14] $[(py)_3Tm(SPh)_3]_2$,[12] and $(py)_3Yb(SPh)_3$[15]) and because both coordination number and ancillary ligands have a significant impact on Ln−S bond

(12) Lee, J.; Freedman, D.; Melman, J.; Brewer, M.; Sun, L.; Emge, T. J.; Long, F. H.; Brennan, J. G. *Inorg. Chem.* **1998**, *37*, 2512.
(13) Shannon, R. D. *Acta Crystallogr. A* **1976**, *32*, 751.
(14) Mashima, K.; Nakayama, Y.; Shibahara, T.; Fukumoto, H.; Nakamura, A. *Inorg. Chem.* **1996**, *35*, 93.

lengths. Most uncomplicated is the comparison between the $[(py)_3Tm(SPh)_3]_2$ and $(py)_4Yb(SC_6F_5)_3$, given that both compounds are seven-coordinate structures with neutral pyridine donor ligands and no Ln−F interactions, and the effect of Ln substitution is a uniform reduction of all bonds (0.01 Å) for the smaller Yb(III) ion (0.02 Å, if we use the difference in average Tm−N and Yb−N distances to approximate the effective change in Ln radii). Terminal Ln−S bond lengths of 2.706(5) Å in the Tm compound and 2.765(2) Å in the Yb compound indicate that fluorination effectively increases the Ln−S bond length by about 0.05 Å.

While there are significant differences between the shortest and longest Ln−S bonds in the structures of molecular **2**, **3**, **4**, and **6**, there is no clear trend that would indicate that bond lengths are directly related to geometry, as has been noted in the structures of octahedral tris-thiolate compounds in the literature.[15,16] In **2**, the three thiolate ligands are arranged such that S2 and S3 are maximally apart (S2−Ho−S3, 163.92°; S1−Ho−S2, 111.24(6)°; S1−Ho−S3, 98.54(4)°), and the longest Ho−S bond is to S1. The Ho−S bond lengths are essentially equal, with the difference between the shortest and longest Ho−S bond being only 0.013 Å. Such structural features are entirely compatible with ionic bonding models, which would predict that all Ln−S bonds should be equal, and that any bond length inequivalence would have origins in the unequal ligand−ligand repulsive interactions (i.e., in **1**, where S1 is close to the other two thiolates, and thus should be slightly distanced because of the additional anion−anion repulsions).

A similar arrangement of thiolates is found in the Er−DME complex **6**, where two thiolates are further apart (S2−Er−S3a, 145.31(3)°; S1−Er−S2, 93.19(3)°; S1−Er−S3a, 97.99(5)°). There is a slightly greater range of Er−S bond lengths relative to **3** (by inference, given isostructural **2**), with the difference between smallest and largest Er−S bond being 0.029 Å. In this compound, however, the longest bond (Er−S2) is not found at the ligand site with the greatest anion−anion repulsions (S1).

Eight-coordinate **4** has a slightly different arrangement of anionic ligands, with S2 considerably apart from S1 and S3 (S1−Sm−S3, 86.16(8)°; S1−Sm−S2, 122.21(8)°; S2−Sm−S3 146.95(7)°). There is also a more dramatic spread of Sm−S bond lengths (0.058 Å) in the molecule, with the longest bond going to the anion with the least ligand−ligand repulsions. Finally, the anion arrangement in seven-coordinate **5** is similar to that in **4**, although with no Yb−F interaction **5** adopts a nearly ideal pentagonal bipyramidal geometry with axial pyridine ligands and three equatorial thiolates. Both pyridine compounds **4** and **5** have a similar range of metal−sulfur bond lengths (Yb, 0.054 Å; Sm, 0.058 Å). Even so, in contrast to **4**, the bond to the relatively isolated S1 (S1−Yb−S2, 141.42(4)°; S1−Yb−S3, 153.45(4)°; S2−Yb−S3, 65.12(4)°) is one of two essentially equal Yb−S bonds in the molecule (Yb−S1, 2.778(1) Å; Yb−S2, 2.781(1) Å; Yb−S3, 2.727(1) Å), while the chemically equivalent Yb−S bonds (if one ignores $\pi$ stacking interactions) represent the shortest and longest Yb−S bond lengths in the structure. Clearly, directional bonding is absent in these compounds, and factors other than Ln−S covalent bonding have the most significant impact on the length of the Ln−S bond.

Isolation of the Yb(III) compound **5** allows for an examination of the effect fluoro substitution has on the energy of S to Ln(III) charge transfer processes. Absorption maxima for both $Yb(SPh)_3$ ($\lambda_{max}$ = 470 nm)[15] and $Yb(2\text{-}S\text{-}NC_5H_4)_3$ ($\lambda_{max}$ = 388 nm)[17] in pyridine have been recorded, and the absorption maximum of the fluorinated derivative **5** ($\lambda_{max}$ = 440 nm) reveals that $SC_6F_5$ shifts the LMCT excitation to higher energy relative to SPh, but this excitation is lower in energy than the absorption of the corresponding pyridinethiolate compound. Relatively stable Ln(III) ground states of the fluorinated and pyridinethiolate molecules have a dramatic impact on chemical reactivity. For example, elemental S reacts with $Ln(SPh)_3$ to form sulfido clusters[18] with the reductive elimination of PhSSPh, but there does not appear to be any reaction between S and either $Yb(2\text{-}S\text{-}NC_5H_4)_3$ or $Yb(SC_6F_5)_3$. In order to prepare chalcogenido clusters with fluorinated thiolate ligands, heteroanion synthetic methods[19] must be developed further.

## Conclusion

The Ln−F dative interaction in $Ln(SC_6F_5)_3$ compounds is surprisingly prevalent and can persist in the presence of donor ligands as basic as pyridine. While there is a clear tendency for F to coordinate to Ln as the size of the Ln radius increases, an absolute correlation between ionic size and the number of Ln−F bonds does not exist because these bonds are particularly susceptible to external influences such as crystal packing effects. Structure, solubility, and electronic properties are all clearly impacted by the electron-withdrawing nature of the fluoride ligands. Chemically, the fluoride substituents render these compounds unreactive toward elemental chalcogen.

**Acknowledgment.** This work was supported by the National Science Foundation under Grant CHE 9982625.

**Supporting Information Available:** X-ray crystallographic files in CIF format for the crystal structures of **1**, **2**, **4**, **5**, and **6**. This material is available free of charge via the Internet at http://pubs.acs.org.

IC0104813

(15) Lee, J.; Brewer, M.; Berardini, M.; Brennan, J. *Inorg. Chem.* **1995**, *34*, 3215.

(16) (a) Freedman, D.; Melman, J.; Emge, T. J.; Brennan, J. G. *Inorg. Chem.* **1998**, *37*, 4162. (b) Aspinall, H.; Cunningham, S. A.; Maestro, P.; Macaudiere, P. *Inorg. Chem.* **1998**, *37*, 5396.

(17) Berardini, M.; Lee, J.; Freedman, D.; Lee, J.; Emge, T. J.; Brennan, J. G. *Inorg. Chem.* **1997**, *36*, 5772.

(18) (a) Freedman, D.; Emge, T. J.; Brennan, J. G. *J. Am. Chem. Soc.* **1997**, *119*, 11112. (b) Melman, J. H.; Emge, T. J.; Brennan, J. G. *Inorg. Chem.* **1999**, *38*, 2117. (c) Melman, J. H.; Emge, T. J.; Brennan, J. G. *Chem. Commun.* **1997**, 2269.

(19) (a) Melman, J. H.; Fitzgerald, M.; Freedman, D.; Emge, T. J.; Brennan, J. G. *J. Am. Chem. Soc.* **1999**, *121*, 10247. (b) Kornienko, A.; Melman, J.; Emge, T.; Brennan, J. *Inorg. Chem.*, in press.